

Flying Sensors: merging Nano-UAV with Radiofrequency Identification

Michela LONGHI and Gaetano MARROCCO

Abstract—The concurrent evolutions of micro/nano Unmanned Aerial Vehicles (UAVs) and sensor-oriented Radio frequency identification (RFID) technology, prompts the idea of *winged-tags* for an ubiquitous and dynamic monitoring of harsh environments and of large indoors spaces.

It is here described and experimentally characterized the concept of *Tag-Drone* comprising a low-cost nano-quadcopter and a miniaturized RFID tag having temperature sensing capability. The weight of the RFID sensor is compatible with the modest payload of the quadcopter and it can be interrogated up to three meters. A simple experimental procedure, involving a reproducible guided flight of the *Tag-Drone*, is hence described to estimate the *visibility time windows* with respect to a base station for on-the-flight data exchange in case of different operational modes.

Index Terms—Radio Frequency Identification, RFID, wireless sensor, nano-drone, UAV, UHF antennas, RFID sensors.

I. INTRODUCTION¹

Radio frequency identification (RFID) is gathering interest in the emerging disciplines of Smart City [1] and Internet of Things [2]. This technology looks promising to create a pervasive network of low-cost sensors able to measure ambient parameters and provide useful data in case of risky conditions, as well as to prevent dangerous events and manage post-disaster scenarios. Sometimes, RFID sensors are required to be placed into non easily reachable harsh environments [3], for example in case of chemical pollution [4], radiations [5], high temperatures, mining industry [6], [7], ravines and steep areas.

Concurrently, there is a wide-spreading growth of Unmanned Aerial Vehicles (UAV) also involving low-cost micro/nano-drones with a very limited battery autonomy but able of indoor flight and to reach dangerous places where humans cannot operate in safety conditions.

RFID and UAV technologies are being already mixed to provide the interrogation of sensor tags displaced over the earth by means of a reader installed onboard the UAV, for application to Structural Health Monitoring [8], [9], Safety of Constructions [10], [11], Precise Agriculture, Automated Inventory in large areas [12], Animal Surveillance [13] and Environmental Preservation [14]. The flight altitude can be properly chosen [15] for the purpose of maximizing the

¹Authors are with the Pervasive Electromagnetic Lab (www.pervasive.ing.uniroma2.it) at the University of Roma Tor Vergata, via del Politecnico, 1, 00133 Roma, Italy. Corresponding email addresses: michela.longhi@uniroma2.it and gaetano.marrocco@uniroma2.it.

interrogation footprint at ground level in correlation with the several system parameters.

This paper addresses a different architecture of combined RFID-UAV systems involving a RFID sensor that is now hosted onto a nano-drone in order to exploit the idea of *winged RFID sensor* (Fig. 1). This is to say that the sampling point is made dynamic as the sensor tag is allowed to move in the environment, where needed, and to bring back the measured data. The resulting *Tag-Drone* could be hence able to reach and stay in a fixed position of the harsh place, as well as to collect a three-dimensional map of any environmental parameter (e.g. temperature, brightness, humidity, pollution) by flying within a given indoor volume as in airports, stations, farms and cold storage warehouses. The same equipment will be moreover useful in restricted critical cases e.g. in the event of fire, gas leak and biological weapons. A critical issue is however the data exchange, possibly on-flight, with a base station.



Figure 1. Pictorial concept of a *Tag-Drone* flying and making measurements within indoor harsh environments.

We are going to introduce a first version of RFID sensor tag suitable to be integrated with a small and low-cost quadcopter to sample physical parameters. The antenna of the tag is an asymmetric dipole made of a T-shaped profile connected to a small rectangular ground plate for a reliable application over plastic or composite chassis of the quadcopter. The device may work in both battery-less and battery-assisted modes and can be read up to 3.5m. Then, the on-the-flight RFID link is experimentally characterized by means of prototypes, for the purpose to identify the useful visibility time window when

the Tag-Drone approaches a potential base station for data upload/download.

II. TAG-DRONE ANTENNA

Without loss of generality, the reference UAV platform for the antenna design and experimentations is the Crazyflie 2.0 nano-drone (Fig. 2). It is an open source device, equipped with Bluetooth LE radio that makes it easy to be controlled directly by a fixed computer (by means of a joystick) using a USB 2.4GHz dongle or even by a smartphone hosting a dedicated app. The quadcopter is made of a unique cross-shaped PCB of 9cm maximum size (motor to motor), with a takeoff weight of 42g. The flight autonomy is up to 7 minutes and the payload is 15g. The RFID tag will be hosted in the central portion of the drone, within a $3 \times 3 \text{cm}^2$ area.



Figure 2. The Crazyflie 2.0 reference quadcopter with indication of the place where the tag antenna will be placed.

The considered antenna layout is shown in Fig. 3 and comprises a T-shaped monopole, vertically connected to a small ground plane at the purpose to both increase the electrical length of the antenna and to provide a few electrical decoupling with the drone electronics.

The antenna is connected to the AMS-SL900A IC transponder capable of on-chip temperature measurement (range: -40°C to 125°C , typical resolution 0.1°C , depending on the range) and providing other pins for interconnection of additional resistive/capacitive sensors as well as of a battery for data-logger mode. The declared input impedance is $Z_{chip} = (123 - j303)\Omega$ and the power sensitivity $P_c = -6.9 \text{dBmW}$ in passive mode and $P_c = -15 \text{dBmW}$ when it is used in BAP (Battery-Assisted) mode.

Designing an antenna for this specific IC deserves some care as it can not be connected to a closed conducting path like the conventional T-match transformers. Accordingly, the reactance matching is achieved by the use of a lumped inductor placed between the chip and the antenna. The width b of the horizontal stripe affects the input resistance of the antenna and, once fixed the tuning inductor ($L_T = 62 \text{nH}$), the length a of the horizontal strip is varied to achieve a fine tuning at the European frequency $f_0 = 870 \text{MHz}$.

The layout was simulated by the Finite-Difference Time-Domain method through the CST - Microwave Studio solver. Due to the small size of the antenna and of the expected narrow bandwidth, the numerical simulation includes a real inductor

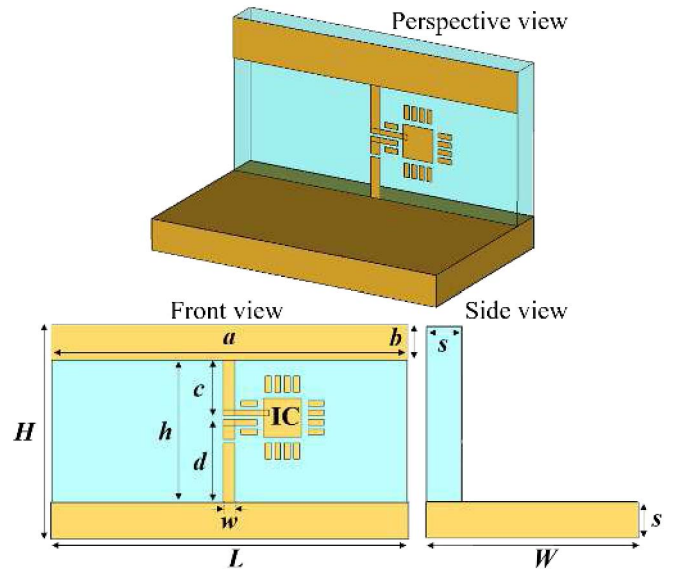


Figure 3. T-shaped tag layout with finite ground plane. Size: $a = 30 \text{mm}$; $b = 3 \text{mm}$; $c = 4.7 \text{mm}$; $d = 7 \text{mm}$; $w = 1 \text{mm}$; $H = 18 \text{mm}$; $L = 30 \text{mm}$; $W = 15 \text{mm}$; $s = 3 \text{mm}$.

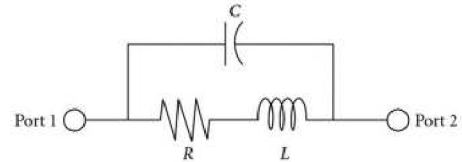


Figure 4. The real inductor schema.

model (Fig. 4) with the purpose to properly account for the frequency detuning due to non-ideal effects. The equivalent parasitic capacitance and resistance

$$C(f) = \frac{1}{(2\pi f_{sr})^2 L_T}, \quad R(f) = \frac{2\pi f L_T}{Q(f)}, \quad (1)$$

are derived by the the self-resonance frequency f_{sr} and by the quality factor Q provided by the inductor manufacturer (Murata [16]).

The radiation pattern of the tag-under-drone (Fig. 5) is rather similar to that of a small dipole. The power transfer coefficient (Fig. 6a) exhibits a modest peak ($\tau = 0.6$), mostly related to the rather high value of the input resistance of the chip that can not be adequately matched by the much lower antenna resistance ($R_A = 31\Omega$) due to its small size. Accordingly, the realized gain along the horizontal plane (Fig. 6b) is $\bar{G} = G\tau = -3.2 \text{dBi}$.

III. PROTOTYPES

Prototypes (Fig. 7) were manufactured with carved copper traces, by means of a digital-controlled plotter, stuck over a $30 \times 15 \times 3 \text{mm}^3$ slab of PVC (Polyvinyl chloride, with permittivity $\epsilon_{PVC} = 1.55$), and connected to an identical fully copper-coated slab, to form an ‘‘L-corner’’.

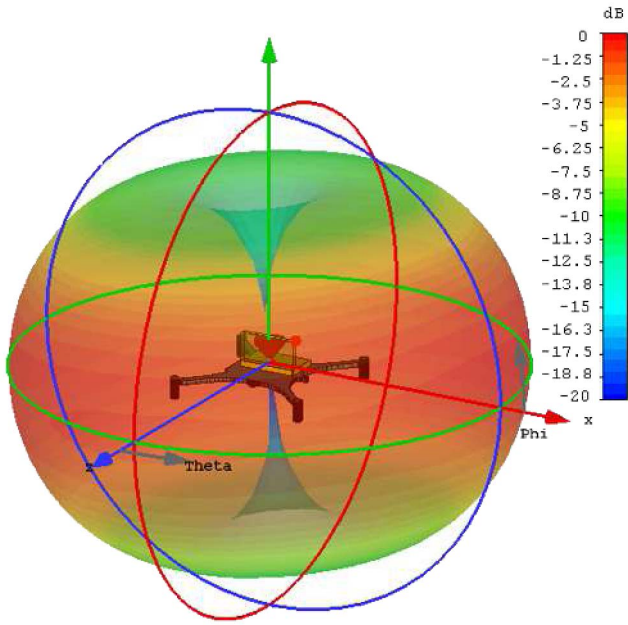


Figure 5. Simulated Radiation gain pattern of the antenna placed under the quadcopter at $870MHz$.

The overall weight of the tags is $2.3g$ and $3.4g$ for battery-less and battery-equipped configurations, respectively, which seem compatible with the drone payload ($15g$).

The tag was hence mounted underneath the quadcopter (looking toward ground) and the resulting object was characterized in a semi-anechoic environment (Fig. 8). The device was illuminated by a folded patch antenna (maximum gain $G_R = 5dBi$) connected to a ThingMagic M6e reader. The realized gain of the tag was hence estimated by means of the turn-on method [17], i.e. following the measurement of minimum power the reader has to emit in order to activate the tag, frequency by frequency, from a given distance. The results (Fig. 9) are in reasonable agreement with the simulation especially around the $f = 870MHz$ frequency where the antenna had been specifically optimized. The estimated maximum free-space read range is $1.5m$ in case of battery-less mode and up to $3.5m$ in case the battery-assisted mode was enforced.

IV. CHARACTERIZATION OF THE ON-THE-FLIGHT RFID LINK

The communication link between the flying Tag-Drone and a fixed base station is here characterized by means of an indoor experiment aimed at identifying the *visibility time-window*, i.e. the time interval wherein the reader is capable of establishing a communication with the flying tag. The visibility time-window is expected to depend on the velocity of the Tag-Drone and on its distance from the reader.

Due to the poor control over the nano-drone motion (no GPS, neither any other assistive positioning system are available) and to the corresponding difficulty to follow and, above all, to reproduce a given trajectory, a custom measurement set-up was arranged. The nano-drone was constrained to fly along

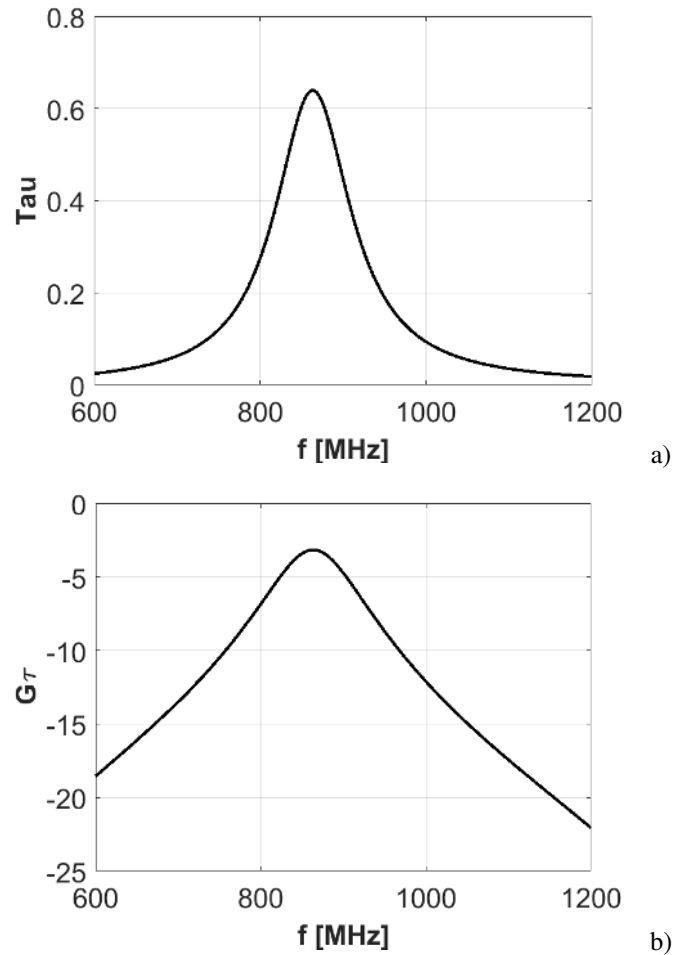


Figure 6. The simulated a) power transfer coefficient and b) the realized gain of the tag antenna when mounted onboard the nano quadcopter.

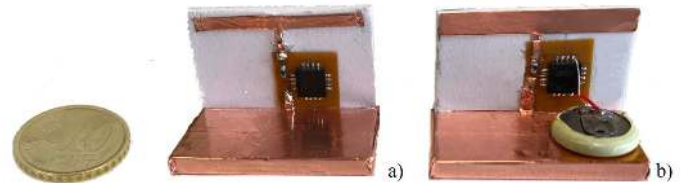


Figure 7. Prototypes of the nano-drone sensor-tag with and without a 3V battery for passive and battery-assisted operations.

two parallel canvas wire-rails (Fig. 10) from the floor to the ceiling of a room for an overall useful path of $2.65m$. The interrogating reader was placed in front of the rails, at $85cm$ from the ground: as the Tag-Drone moves uphill and downhill, it will change only one coordinate with respect to the reader's antenna and a repeatable measurement can be achieved. By assuming a 90° rotation (so that the Tag-Drone now translates parallel to the ground), this arrangement could emulate a possible flying path of the Tag-Drone across a gate with the purpose of data exchange. The experiment was repeated for several mutual reader-drone (rails) distances $d_{RD} = \{30cm,$

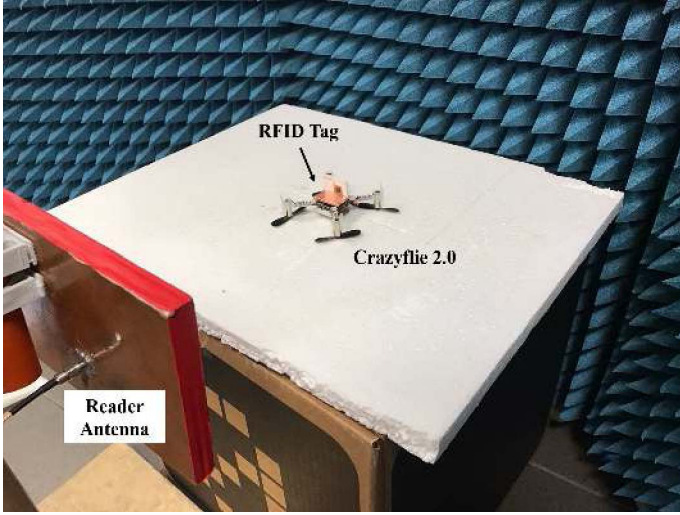


Figure 8. Measurement set up comprising an interrogating linear patch antenna (max gain $5dBi$) connected to the Thing-Magic M6e reader. The sensor-tag onboard the nano-drone was positioned at $30cm$ distance from the antenna.

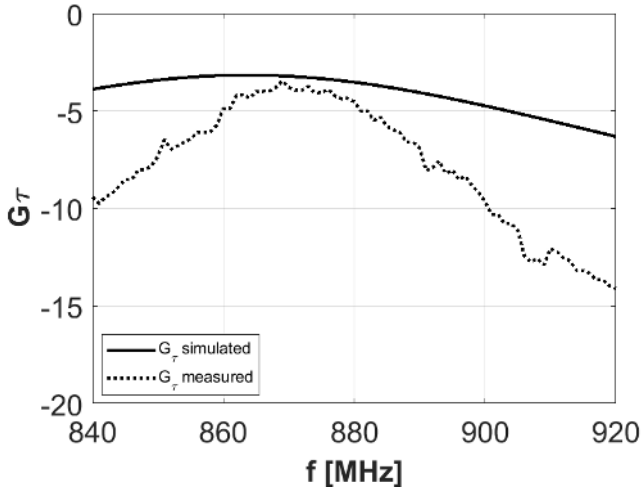


Figure 9. Measured and simulated realized gain of the Tag-Drone in frontal direction.

$40cm, 1m, 1.6m$ } and for three different speeds $v = \{0.05m/s$ (Slow), $0.13m/s$ (Medium), $0.5m/s$ (Fast)}. The reader returned the collected RSSI that is proportional to the back-scattered power.

Fig. 11a shows an example of RSSI traces, for four reader-rails distances and the battery-less nano-drone flying, at velocity $v = 0.05m/s$, from floor to ceiling (A-B-C) and then from ceiling down to the floor (C-B-A). The typical bell-shaped profiles permits to extract the visibility time-windows Δt that are summarized, for all the considered cases, in Table I. In spite of the rough manual control of the flight parameters, the values are rather similar for uphill and downhill paths. The useful visibility-time of the tag by the reader is obviously related to the mutual tag/reader distance and dramatically reduces with the velocity. With reference to a tag/reader

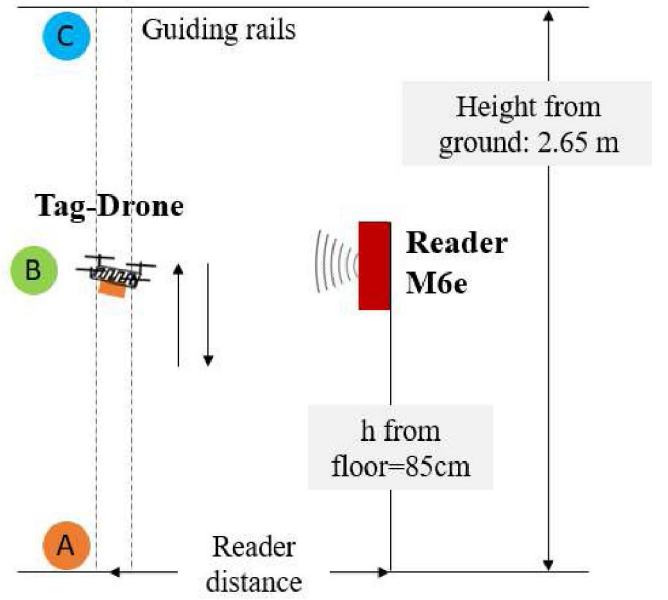


Figure 10. Schematic of the experimental setup for the evaluation of the RFID link by a flying tag constrained to move along vertical wired rails.

distance of $1m$ (Fig. 11b), the visibility time-window spans between $1.5s \leq \Delta t \leq 16s$. Such numbers have to be referred to the typical time ($T_d = 2 \div 3s$) required by the reader to download the data from a sensor tag working in data-logging mode. The communication between the interrogator and tag can indeed occurs only if the visibility of the electromagnetic device is $\Delta t > T_d$, i.e. the velocity $v = 0.13m/s$ has to be considered an upper bound, at least for the experimented distances.

	30cm		40cm		1m		1.6m	
	Up	Down	Up	Down	Up	Down	Up	Down
slow	19.8s	15.3s	20.7s	19.6s	15.6s	17.4s	15.6s	12.7s
med	6.2s	6.9s	6.3s	7.3s	5.4s	7s	5.7s	5s
fast	1.4s	1.5s	1s	1.6s	1.5s	1.3s	1s	1s

Table I
DURATION OF THE VISIBILITY WINDOWS Δt OF THE BATTERY-LESS TAG-DRONE WITH RESPECT TO A FIXED READER FOR DIFFERENT DISTANCES READER/RAILS AND AND QUADCOPTER SPEEDS.

V. CONCLUSIONS

We have presented a first proof of concept of Tag-Drone comprising an ad-hoc designed small sensor-tag mounted onboard a nano-drone quadcopter. The resulting device, even if still open to improvements, allows a read range up to $3.5m$.

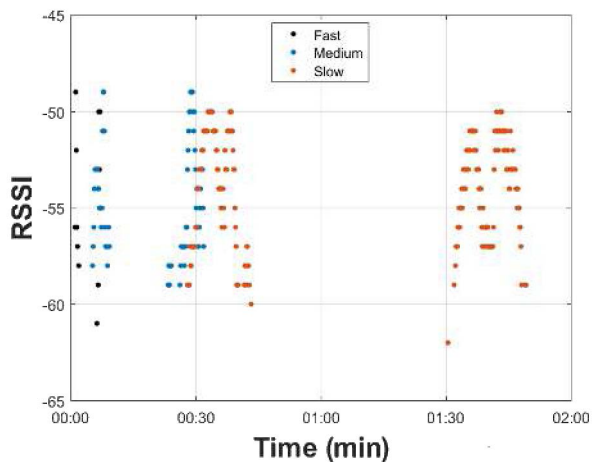
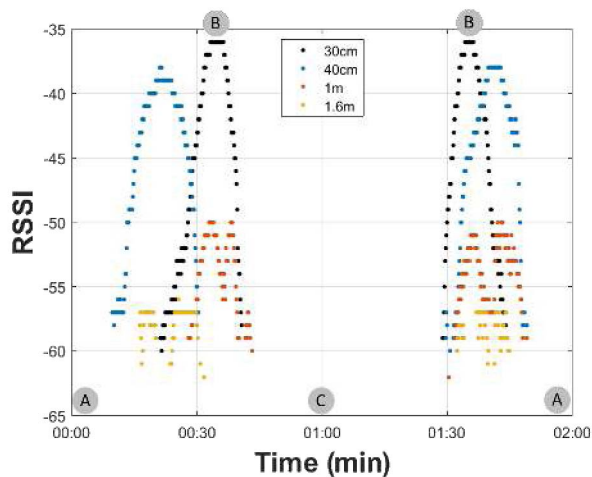


Figure 11. The RSSI values returned by the battery-less Tag-Drone flying along the guiding rails from the floor (position A), up to the ceiling (position C), passing in front of the reader's antenna (position B) where the RSSI peak occurs, and downhill. a) Fixed velocity $v = 0.05m/s$ and different reader-rails distances; b) fixed reader-rails distance $d = 1m$ and different speeds.

An experimental setup to achieve reproducible assisted-flights permitted the characterization of the RFID link for an on-the-flight data exchange with a fixed base station that looks compatible with a velocity up to $v = 0.13m/s$ ($0.5km/h$).

Future research will be devoted to the improvement of the tag's antenna performance and to the integration of the battery within a compact design and hence to some experimentations in realistic conditions.

The achieved results are anyway encouraging and, thanks to the highly reducing cost of nano-drones, it is not infeasible to imagine a possible new generation of disposable augmented UAVs becoming the flying and ubiquitous version of nowadays RFID sensor devices.

REFERENCES

[1] N. Komninos, "Intelligent Cities, Innovation, Knowledge Systems, and Digital Spaces," Book, London, U.K.: Spon Press London, 2003.

[2] L. Atzori, A. Iera, G. Morabito, "The Internet of Things: a Survey," *Computer Networks*, vol. 54, no. 15, pp. 2787–2805, Oct. 2010.

[3] G. Greco, C. Lucianaz, S. Bertoldo, M. Allegritti, "A Solution for Monitoring Operations in Harsh Environment: a RFID Reader for Small UAV," In *Electromagnetics in Advanced Applications (ICEAA)*, 2015 International Conference, pp. 859-862, Sept. 2015. DOI: 10.1109/ICEAA.2015.7297235

[4] M. A. Kovacina, D. Palmer, G. Yang, R. Vaidyanathan, "Multi-Agent Control Algorithms for Chemical Cloud Detection and Mapping Using Unmanned Air Vehicles," *IEEE/RSJ International Conference on Intelligent Robots and Systems*, Sept. 30 2002-Oct. 4 2002.

[5] J. Han, Y. Xu, L. Di, Y.Q. Chen, "Low-cost Multi-UAV Technologies for Contour Mapping of Nuclear Radiation Field," *Journal of Intelligent & Robotic Systems*, April 2013, vol. 70, pp. 401–410, Apr. 2013.

[6] S. Lee, Y. Choi, "Reviews of Unmanned Aerial Vehicle (drone) Technology Trends and Its Applications in the Mining Industry," *Journal of Geosystem Engineering*, vol. 19, no.4, pp. 197-204, Mar. 2016.

[7] M. Shahbazi, G. Sohn, J. Théau, "UAV-based Point Cloud Generation for Open-Pit Mine Modeling," *International Conference on Unmanned Aerial Vehicles in Geomatics*, 30 Aug–02 Sep 2015, Toronto, Canada.

[8] D. Levin, "Futuristic Inspections for Bridge Safety," in *TuftsNow*, Tufts University, May 2014. Available: <http://now.tufts.edu/articles/futuristic-inspections-bridge-safety>

[9] D. Mascarenas, E. Flynn, M. Todd, G. Park, C. Farrar, "Wireless Sensor Technologies for Monitoring Civil Structures," *Sound and Vibration*, no. 42, pp. 16-21, Apr. 2008.

[10] M. Gheisari, J. Irizarry, B.N. Walker, "UAS4SAFETY: The potential of unmanned aerial systems for construction safety applications," *Construction Research Congress 2014: Construction in a Global Network*, ASCE, pp. 1801–1810.

[11] B. Hubbard, H. Wang, M. Leasure, T. Ropp, "Feasibility Study of UAV use for RFID Material Tracking on Construction Sites," In Proc., *ASCE Annual International Conference*, 2015, pp. 669-676.

[12] "The flying inventory assistant," *Fraunhofer Institute for Material Flow and Logistics IML*, Dec. 2014. Available: <https://www.fraunhofer.de/en/press/research-news/2014/december/the-flying-inventory-assistant.html>

[13] "Kenyan Reserve Sheltering Rare Rhinos to Launch Antipoaching Drone," *Wired Technology*, Jul. 2013. Available: <http://www.wired.co.uk/news/archive/2013-07/29/anti-poaching-drone-kenya>

[14] M. Allegritti, S. Bertoldo, "Recharging RFID Tags for Environmental Monitoring Using UAVs: A Feasibility Analysis," *Wireless Sensor Network*, vol.7, no.2, pp. 13-19, Feb. 2015.

[15] M. Longhi, G. Casati, D. Latini, F. Carbone, F. Del Frate, G. Marrocco, "RFIDrone: Preliminary Experiments and Electromagnetic Models," *URSI International Symposium on Electromagnetic Theory (EMTS)*, Espoo, Finland, Aug. 2016. DOI: 10.1109/URSI-EMTS.2016.7571423

[16] MURATA, <http://www.murata.com/products/inductor>.

[17] "Self-sensing Passive RFID: From Theory To Tag Design and Experimentation," *European Microwave Conference, EuMC 2009*, Roma, Italy, 2009.